Available online at www.sciencedirect.com
SCIENCE DIRECT®
Chemical Physics Letters 418 (2006) 442–447
CHEMICAL PHYSICS LETTERS
www.elsevier.com/locate/cplett

Contribution of two-photon and excited state absorption in 'axial-bonding' type hybrid porphyrin arrays under resonant electronic excitation

P. Prem Kiran [a,c,*], D. Raghunath Reddy [b], A.K. Dharmadhikari [c], Bhaskar G. Maiya [b], G. Ravindra Kumar [c], D. Narayana Rao [a]

[a] School of Physics, University of Hyderabad, Hyderabad 500 046, India
[b] School of Chemistry, University of Hyderabad, Hyderabad 500 046, India
[c] Tata Institute of Fundamental Research, 1 Homi Bhabha Road, Mumbai 400 005, India

Received 7 October 2005; in final form 26 October 2005
Available online 21 November 2005

Abstract

Two-photon absorption (2PA) and excited state absorption (ESA) properties of 'axial-bonding' type hybrid porphyrin arrays are investigated in the picosecond regime under single-photon resonant excitation condition. A crossover from reverse saturable absorption (RSA) to saturable absorption (SA) and back to RSA is observed with the increase of excitation intensity. In the corresponding intensity ranges, third- and fifth-order phase conjugate signals from degenerate four wave mixing are observed. These observations are explained using rate equations for population densities in a three-level energy scheme. At higher intensities, 2PA is found to be dominant contributor to nonlinear absorption compared to ESA.

1. Introduction

Organic materials with delocalized electrons have attracted basic as well as applied research because of their large nonlinear optical susceptibilities, architectural flexibility, and ease of fabrication. The delocalization of an electron in the molecular frame enhances the optical nonlinearity and this has been one of the most successful strategies for improving nonlinearity. The optical and electronic properties of many oligomeric conjugated systems have been investigated to determine structure–property relations [1] focusing on the third-order nonlinear optical susceptibilities ($\chi^{(3)}$) [2,3]. Conjugated organic materials have been widely investigated in search of suitable chromophores for all-optical applications like switching and limiting [4]. Metalloporphyrin and metallophthalocyanines form an important class of electronic materials exhibiting nonlinear absorption, due to their large π-electron conjugation, high values of $\chi^{(3)}$ and small HOMO–LUMO gaps with two-dimensional conjugated molecular structure [5–7]. The architectural flexibility like axial substitution of heavy atom and electron-donor subunits linked to the central metal atom [8–10] in porphyrins provides extra ways of optimizing the nonlinear absorption (NLA).

Excited state absorption (ESA) and two-photon absorption (2PA) are the important processes leading to NLA behaviour in metalloporphyrins. Linear absorption in a chromophore is a $\chi^{(1)}$ process and ESA is a sequential $\chi^{(1)}$:$\chi^{(1)}$ process effectively giving rise to third-order nonlinearity. 2PA itself is a $\chi^{(3)}$ process involving four fields. An electronic nonlinear optical process is said to be resonant when the excitation wavelength is closer to any absorbing electronic transition. Under resonant and near resonant excitations, ESA is the dominant mechanism in metalloporphyrins [11], whereas, under nonresonant excitation

* Corresponding author.
E-mail address: prem@tifr.res.in (P.P. Kiran).

0009-2614/$ - see front matter © 2005 Elsevier B.V. All rights reserved.
doi:10.1016/j.cplett.2005.10.139

2PA dominates the NLA behaviour [11–13]. Under certain excitation conditions, both ESA and 2PA may be operative simultaneously leading to higher nonlinearities [14]. In this Letter, we discuss the contribution of ESA and 2PA to the NLA with increasing excitation intensity in 'axial-bonding' type hybrid porphyrin arrays based on tin(IV) tetratolylporphyrin (Sn^{IV}TTP) scaffold under resonant excitation. We present observations of open aperture *Z*-scan technique and degenerate four wave mixing (DFWM) in the picosecond (ps) regime and attribute the observed NLA to third- and fifth-order optical nonlinearities to the excited states of the molecules.

2. Axial-bonding type hybrid Sn^{IV}TTP arrays

Monomer and dimers are synthesized following the procedure reported in the literature [15]. The nomenclature of monomer molecule is *meso*-5,10,15,20-(tetratolyl) porphyrinato tin(IV) dihydroxide; [(TTP)$Sn^{IV}(OH)_2$]; and is represented as SnTTP in this Letter. The architecture of the trimer arrays is such that Sn^{IV} complex of *meso*-5,10,15,20-(tetratolyl)porphyrin forms the basal scaffolding unit, and free-base, Ni^{II} porphyrins occupy the two axial sites via an aryloxy bridge [16]. The nomenclature of trimer arrays is: (free-base porphyrin)$_2$(tin(IV)porphyrin) ≡ [(TTP)-$Sn^{IV}(H_2TriTP(O))_2$] and (nickel(II)porphyrin)$_2$ (tin(IV)porphyrin) ≡ [(TTP)-$Sn^{IV}(NiTriTP(O))_2$] and are represented as Sn-$(H_2)_2(TTP)_3$ and Sn-$Ni_2(TTP)_3$, respectively. The molecular structures of monomer and trimer are shown in Fig. 1a. The dimer molecule has two monomers linked covalently at *meso* position with ethoxy spacer. The nomenclature of the tin(IV) dimer is [μ-[5,10,15-tri (*p*-tolyl)-20-[4-[2-[4-[10,15,20-tri(*p*-tolyl)-5-porphyrinyl]phenoxy]ethoxy]phenyl]porphyrinato]]di(tin)(IV)tetrahydroxide; [(TriTP)-$Sn^{IV}(OH)_2$]-$O(CH_2)_2O$-(TriTP)$Sn^{IV}(OH)_2$] and is represented as Sn-Sn$(TTP)_2$. The architecture of hexamers [15] is based on a covalently linked Sn^{IV} porphyrin dimer, with each of the two Sn^{IV} porphyrins centers *trans*-axially ligated to two free-base, zinc(II) tetratolylporphyrins. The nomenclature of the hexamers is: [(TTP)-$Sn^{IV}(H_2TriTP(O))_2$]-$O(CH_2)_2O$-[(TTP)-$Sn^{IV}(H_2TriTP(O))_2$] and [(TTP)-$Sn^{IV}(ZnTriTP(O))_2$]-$O(CH_2)_2O$-[(TTP)-$Sn^{IV}(ZnTriTP(O))_2$] and are referred as Sn_2-$(H_2)_4(TTP)_6$ and Sn_2-$Zn_4(TTP)_6$, respectively. The molecular structure of dimer and hexamer is given in Fig. 1b.

Representative UV–Vis absorption spectra of the arrays are shown in Fig. 2. The UV–Vis spectrum of a given trimer and hexamer compared to the corresponding monomeric porphyrin suggest that the absorption peaks of these compounds are in the same range, indicating minimal perturbation of the electronic structures of the individual macrocyclic π-systems in these arrays. Minor variations in the spectral features of the trimers with respect to the corresponding monomers are ascribed to the 'substituent effects' [15,16]. On the other hand, the singlet state activities of these oligomers are quite different from those of the precursor reference compounds as probed by steady-state fluorescence and fluorescence lifetime measurements using time correlated single photon counting (TCSPC) technique. Fluorescence lifetimes and the respective yields of these porphyrins in dichloromethane as solvent are given in Table 2. All these molecules have bi-exponential decays for τ_{S1} representing fast and slower decay. It is clear from the Table 2 that as the array becomes larger; the contribution of slowly decaying (long lived) component increases. Longer lifetimes of the first excited singlet state can lead

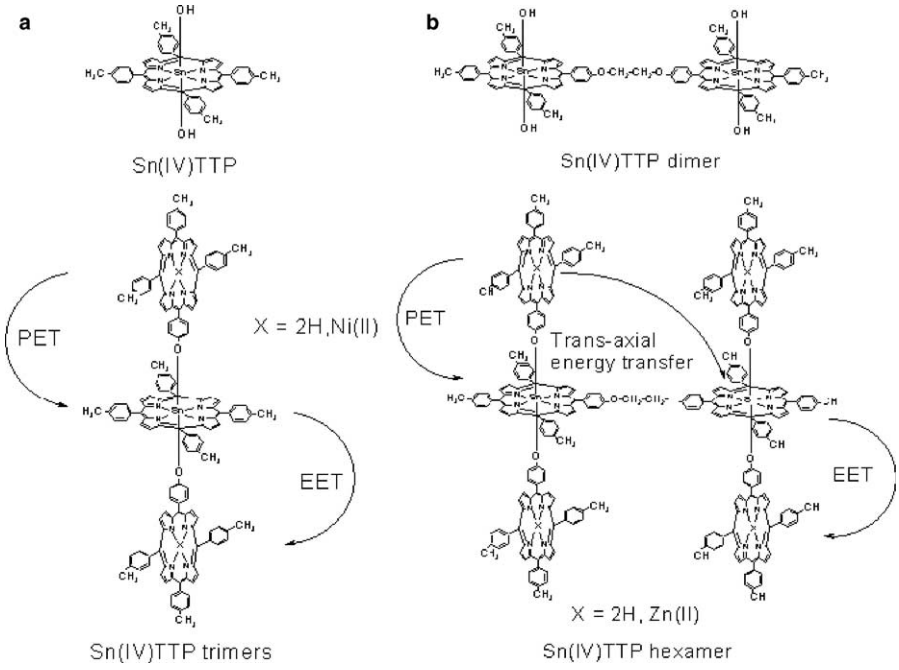

Fig. 1. Molecular structures of: (a) tin(IV) monomer and trimer; (b) tin(IV) dimer and hexamer arrays.

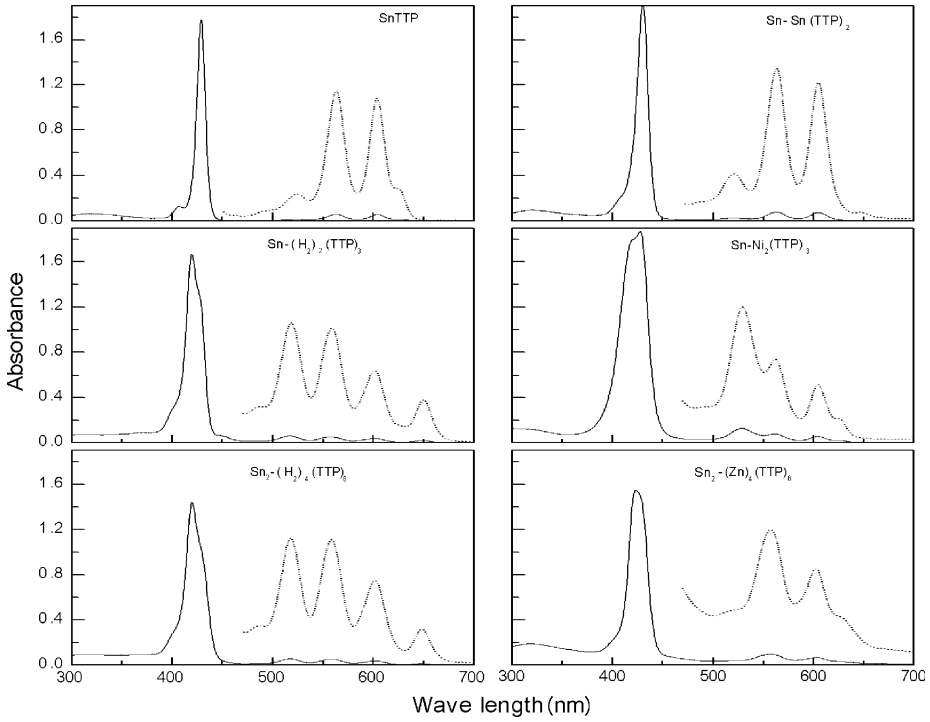

Fig. 2. UV–Vis spectrum of the arrays. Dotted lines are magnified by a factor of 10 for clarity.

to enhanced ESA and subsequently alter the NLA properties of a molecular system. The lifetimes of the first excited singlet state change considerably with substitution of metal in hexamers. Substitution of Zn as central metal atom in porphyrin ring is reported to vary the singlet state properties and triplet state formation quite significantly [17].

3. Experimental details

Second harmonic (532 nm) radiation from a hybrid mode-locked Nd:YAG laser giving 25 ps pulses at 10 Hz repetition rate is used in our studies. Open aperture *Z*-scan [18] is carried out by focusing the input beam on to the sample with linear transmission of ~75% at 532 nm using a lens of 500 mm focal length to 60 μm spot-size at focus giving peak intensities in the range 5–50 GW cm^{-2}. The transmitted light is collected using a photodiode. We have employed the standard backward DFWM phase conjugate geometry [19] for the measurement of $\chi^{(3)}$. Using a beam splitter, a part of the input beam is split and used for the backward pump (beam 3) and is gently focused using a 1000 mm lens. The rest of the beam is again split using a second beam splitter. One part of this beam is the probe (beam 2) that passes through a delay line and meets the forward pump. The other part is the loosely focused (using a 2000 mm focal length lens) forward pump (beam 1) reaching sample at a fixed delay. The spot-size of the beams on the sample is measured to be ~1 mm. The angle between the forward pump and the probe is ~5.1°. A half wave plate (HWP) is introduced in the probe beam to change its state of polarization. A part of the forward pump is picked up by a photodiode to monitor the pulse-to-pulse fluctuations. All the samples, dissolved in chloroform, are placed in a 1-mm quartz cuvette.

4. Nonlinear absorption and optical nonlinearities

The open aperture *Z*-scan curve representing NLA of Sn_2-$Zn_4(TTP)_6$ hexamer is shown in Fig. 3. NLA shows a totally different behaviour with increasing intensity. In the intensity range of 5–10 GW cm^{-2} these oligomers show only RSA due to ESA. With the increase of input intensity to 10–25 GW cm^{-2} we observed SA in RSA due to the saturation of ESA in the $S_1 \rightarrow S_n$ transition. At further higher intensities (35–50 GW cm^{-2}) RSA within saturation of ESA due to 2PA is observed. In Sn-H_2 oligomers initial

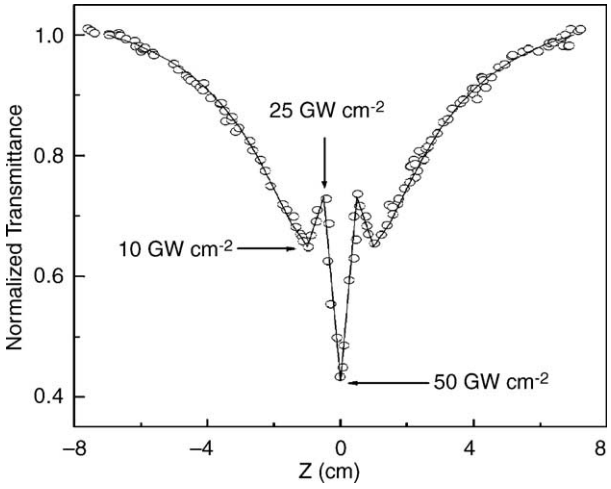

Fig. 3. Open aperture *Z*-scan curve of Sn_2-$Zn_4(TTP)_6$.

RSA is followed by saturation of ESA and no further switchover to RSA is observed even at higher intensities. Such intensity dependent saturation of ESA ($S_1 \rightarrow S_n$) and faster higher excited state relaxation has been observed earlier in axial ligated porphyrins [8,9]. The excitation wavelength 532 nm, lies in resonance with higher levels of the Q-band ($S_0 \rightarrow S_1$ transition) in the arrays having Sn-H_2 porphyrins and is at the absorption edge in the arrays with metal–metal (Sn–Ni, Sn–Sn, Sn–Zn) interactions. Though ESA, 2PA and higher excited state lifetimes appears to play an important role in the nonlinear absorption, 2PA is predominant in oligomers having metal–metal interactions and is essentially negligible in molecules having metal–freebase interaction. Though 2PA process is predominant in non-resonant excitation, large resonant enhancement in the 2PA cross-section can be expected due to stepwise single-photon transition and by proper structural modifications to the porphyrin moiety [13].

In order to investigate the nonlinearities causing the crossover in NLA, we performed DFWM in phase conjugate (PC) geometry. The log–log plot of input energy and PC signal for Sn_2-$Zn_4(TTP)_6$ hexamer is shown in Fig. 4a. These arrays show a slope of ~3 at intensities lower than 10 GW cm^{-2} and above this intensity the slope approaches ~5.2, suggesting higher-order nonlinear contributions. For dimer molecule, higher slope appeared at relatively lower intensities (~9 GW cm^{-2}) compared to that for trimer and hexamers (~15 GW cm^{-2}) arrays. In case

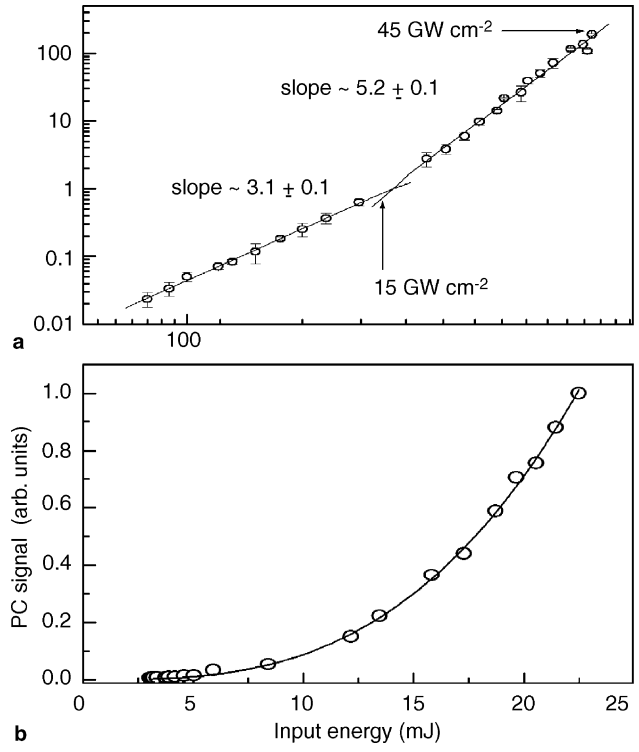

Fig. 4. (a) Log–log plot of PC signal and the input energy for Sn_2-$Zn_4(TTP)_6$. (b) Intensity dependence of the PC signal in $\chi^{(3)}$ measurements for Sn-$Ni_2(TTP)_3$. Line shows the cubic dependence fit.

Table 1
Second hyperpolarizability $\langle\gamma\rangle$ of Sn(IV)TTP oligomers

Porphyrin	$\langle\gamma\rangle$ ($\times 10^{-27}$esu)
Sn(TTP)	0.37×10^{-3} [20]
Sn-$(H_2)_2(TTP)_3$	0.93 ± 0.06
Sn-$Ni_2(TTP)_3$	0.61 ± 0.04
Sn-$Sn(TTP)_2$	3.0 ± 0.20
Sn_2-$(H_2)_4(TTP)_6$	0.33 ± 0.02
Sn_2-$Zn_4(TTP)_6$	0.38 ± 0.03

of Sn–Sn dimer the log–log slope of the phase conjugate signal were 2.8 ± 0.1 and 4.9 ± 0.1 at lower and higher intensities, respectively. However, trimers and hexamers have slopes that are slightly higher than 3 and 5. This can be attributed to additional delocalization of the singlet states in trimers and hexamers due to photoinduced electron transfer (PET) and excitation energy transfer (EET) changing the population densities contributing to nonlinear polarization. Whereas in the case of the dimer, possibility of PET and EET is absent and conjugation via the covalent ethoxy spacer is present.

The second hyperpolarizability $\langle\gamma\rangle$ is measured from cubic dependence of the PC signal (Fig. 4b) and are given in Table 1. The $\langle\gamma\rangle$ value for hexamers and dimer is three and four orders of magnitude larger, respectively, than that of monomers [20]. Excited state enhancements of the optical nonlinearities under resonant excitation are well known in delocalized π-electron systems [21]. The $\langle\gamma\rangle$ is increased from monomer to dimer and then decreases for hexamer arrays. Fig. 4b shows the plot of input energy and the phase conjugate (PC) signal for Sn-$Ni_2(TTP)_3$. The chain length dependence of $\chi^{(3)}$ for several molecular arrays and polymers has been investigated and it is known that the magnitude depends on the number of monomer units [2]. For oligomers of larger monomer unit such as porphyrin, the enhancement of $\langle\gamma\rangle$ is more drastic and it saturates at a much shorter length [22,23]. Deviations from the cubic behaviour of the PC signal with log–log slope approaching ~5, are reported in various porphyrins [20,24].

The four-wave description of the DFWM interaction specifies only the number of beams involved and does not limit the interaction to third-order nonlinearity and depends mainly on the nonlinear mechanism and population densities [25]. In isolated molecules in solution, strongly coupled pairs of excitons created by a 2PA or ESA processes would create a two-photon grating that would produce a scattering proportional to the fifth power of the laser intensity, and an effective $\chi^{(5)}$ process. Similar results of the intensity dependent higher-order nonlinearity [14,26] and absorption [27] are reported in organic materials due to 2PA and 2PA generated ESA. Saturation of the DFWM signal at lower intensities and increase of the slope at higher intensity due to multi-photon ionization processes has been reported in semiconductor materials [24,28] indicating the intensity dependant nonlinearity. Though we have not observed any such saturation of the PC signal in the lower intensity range, the transition from the lower

to the higher intensity regime is fairly continuous. This clearly indicates the presence of ESA in the lower intensity domain and the dominance of 2PA at higher intensities.

We seek to understand our observations using a rate equation model. Since the intersystem crossing from singlet to triplet state is a slower process compared to the excitation pulse width, the generalized five-level model for porphyrin effectively becomes a three-level model involving singlet states S_0, S_1 and S_n. Thus, population distribution in porphyrins can be explained by the rate equations,

$$\frac{dN_0}{dt} = -\frac{\sigma_0 I N_0}{\hbar\omega} - \frac{\beta I^2}{2\hbar\omega} + \frac{N_1}{\tau_1}, \tag{1}$$

$$\frac{dN_1}{dt} = \frac{\sigma_0 I N_0}{\hbar\omega} - \frac{\sigma_1 I N_1}{\hbar\omega} - \frac{N_1}{\tau_1} + \frac{N_n}{\tau_n}, \tag{2}$$

$$\frac{dN_n}{dt} = \frac{\sigma_1 I N_1}{\hbar\omega} + \frac{\beta I^2}{2\hbar\omega} - \frac{N_n}{\tau_n}, \tag{3}$$

and the intensity transmitted through the sample is given by

$$\frac{dI}{dz} = -\sigma_0 I N_0 - \sigma_1 I N_1 - \beta I^2, \tag{4}$$

where N_i and τ_i represents population and the relaxation times of a state S_i, σ_0 is the ground state absorption cross-section from $S_0 \rightarrow S_1$, σ_1 is the excited state absorption cross-section from $S_1 \rightarrow S_n$, β is the 2PA co-efficient, and $\hbar\omega$ is the energy of the excitation photon. I is incident intensity as a function of radial direction (r), time (t), and length (z) of the Gaussian beam. The differential equations are first de-coupled and then integrated over r, t and z within the limits 0 to ∞, $-\infty$ to ∞, and 0 to L (sample thickness), respectively. Typical number of slices used for r, t, and z are 60, 30, and 5, respectively. σ_1, β and τ_{Sn} are estimated through least square fit of the experimental data [29] and are tabulated (Table 2) with the ground and 2PA cross-section (σ_2).

The 2PA cross-section is calculated using $\beta = \frac{N_0}{h\nu}\sigma_2$; [30], where h is the Planck's constant, ν is the frequency of light, and N_0 is the number molecules per unit volume. From Table 2, it is clear that σ_2 is large and comparable with the values reported with dendrimer molecules [31]. Substitution of electron acceptor and donor units is a well known strategy for enhancing the two-photon absorption cross-section in organic molecules [12,32]. A 13-fold enhancement of σ_2 under nonresonant excitation and further enhancement by approaching the one-photon transition is observed in porphyrin with symmetrically substituted electron accepting units [13]. Out of the different oligomers studied, we have observed a nominal 5 times enhancement in σ_2 from SnTTP to Sn-Sn(TTP)$_2$ and Sn_2-Zn_4(TTP)$_6$, whereas Sn-Ni_2(TTP)$_3$ has very large σ_2. This could be due to the contribution of ESA from the highly delocalized singlet states arising due to PET and EET leading to larger resonant 2PA [10].

As the relaxations from the excited singlet state S_n for the arrays having Sn–Sn, Ni, Zn interaction are fast compared to the laser pulse width, the population N_n can be assumed to be constant at very high intensities

$$\text{i.e., } dN_n/dt = 0 \Rightarrow \frac{N_n}{\tau_n} = \frac{\sigma_1 I N_1}{\hbar\omega} + \frac{\beta I^2}{2\hbar\omega}. \tag{5}$$

Substituting this in to Eq. (2), gives

$$\frac{dN_1}{dt} = \frac{\sigma_0 I N_0}{\hbar\omega} - \frac{N_1}{\tau_1} + \frac{\beta I^2}{2\hbar\omega}. \tag{6}$$

The effective population density (N_{eff}) describing the nonlinear polarization (P^{NL}) can be given as,

$$\frac{dN_{eff}}{dt} = \frac{dN_1}{dt} - \frac{dN_0}{dt} = 2\frac{\sigma_0 I N_0}{\hbar\omega} - \frac{1}{\tau_1}\left[N_{eff} + N^0_{eff}\right] + 2\frac{\beta I^2}{2\hbar\omega}, \tag{7}$$

where $N_{eff} = N_1 - N_0$ and $N^0_{eff} = N_1 + N_0$ is the population at zero field, a constant N_0. The resulting P^{NL} can be explained effectively using a two-level system and is proportional to N_{eff}. At higher intensities, the 2PA term has dominant contribution to P^{NL} [33]. Under our DFWM geometry, as both the forward and backward pumps have same intensities, the PC signal will have equal contributions from both the pumps.

The observed fifth-order nonlinearity is considered to be arising from a sequential $\chi^{(3)}$:$\chi^{(1)}$ nonlinearity. Such sequential nonlinearities leading to fifth- and seventh-order nonlinearities are observed in semiconductors [33]. The solid line in Fig. 3 is a theoretical fit to the observed NLA behaviour using the rate Eqs. (1)–(4). For the excitation intensity in the range 10–25 GW cm^{-2} these oligomers show only third-order nonlinearities in DFWM and RSA due to ESA and a crossover from RSA to SA due to the saturation of ESA in the $S_1 \rightarrow S_n$ transition. With further increase in the excitation intensity (35–50 GW cm^{-2}), PC

Table 2
Ground state absorption cross-section σ_0, and excited state parameters, fluorescence lifetimes τ_{S1}, % fluorescence yields σ_1, τ_{Sn} and σ_2 with 25 ps pulse excitation

Porphyrin	τ_{S1} ns, (% fluorescence yield)	σ_0 ($\times 10^{-17}$ cm^2)	σ_1 ($\times 10^{-17}$ cm^2)	τ_{sn} (ps)	σ_2 ($\times 10^4$ GM)
Sn(TTP)	0.56 (71), 1 (28)	0.63	11.60	60	2.7
Sn-$(H_2)_2$(TTP)$_3$	0.74 (71), 5.93 (28)	5.55	1.67	500	–
Sn- Ni_2(TTP)$_3$	0.62 (70), 2.13 (29)	75.00	2.10	50	396.0
Sn-Sn(TTP)$_2$	0.57 (95), 4.94 (5)	21.00	7.00	7.5	13.6
Sn_2-$(H_2)_4$(TTP)$_6$	0.45 (28), 1.95 (23), 7.25 (47)	3.20	1.67	500	–
Sn_2-Zn_4(TTP)$_6$	0.66 (30), 1.73 (69)	5.50	2.30	15	15.7

1 GM = 10^{-50} cm^4 s/photon.

signal shows fifth-order nonlinearities and the contribution of 2PA in RSA is observed.

To summarize, we investigated nonlinear optical properties of porphyrin arrays based on Sn(IV)TTP scaffold under resonant excitation in picosecond timescales. Of all the molecules studied, arrays having metal–metal interactions show higher-order nonlinearities indicating the presence of 2PA associated with ESA process. From the open aperture Z-scan and the DFWM-PC observations, we are able to distinguish clearly the two major contributing processes under resonant intense laser excitation. It is clear that the observed crossover is due to the combined contribution of ESA ($\chi^{(1)}$:$\chi^{(1)}$) involving $S_1 \rightarrow S_n$ and the 2PA ($\chi^{(3)}$ process), with 2PA dominating at higher intensities. Such intensity dependent NLA might have potential applications as a nonlinear optical device in the picosecond domain.

Acknowledgements

Financial support from the Department of Atomic Energy – Board of Research in Nuclear Sciences, and Defence Research Development Organization, India, is acknowledged. P.P. Kiran thanks the Council for Scientific and Industrial Research, India, for the Senior Research Fellowship. Authors thank Dr. Suneel Singh, University of Hyderabad, for discussions with rate equations.

References

[1] P.N. Prasad, D.J. Williams, Introduction to Nonlinear Optical Effects in Molecules and Polymers, Wiley, New York, 1991.
[2] J.L. Bredas, C. Adant, P. Tackx, A. Persoons, B.M. Pierce, Chem. Rev. 94 (1994) 243.
[3] R.R. Tykwinski, U. Gubler, R.E. Martin, F. Diederich, C. Bosshard, P. Gunter, J. Phys. Chem. B 102 (1998) 4451.
[4] G. Horowitz, F. Garnier, A. Yassar, R. Hajaoui, F. Kouki, Adv. Mater. 8 (1996) 52.
[5] P.N. Taylor, J. Huuskonen, G. Rumbles, R.T. Aplin, E. Williams, H.L. Anderson, Chem. Commun. (1998) 909.
[6] T.E.O. Screen, K.B. Lawton, G.S. Wilson, N. Dolney, R. Ispasoiu, T. Goodson III, S.J. Martin, D.D.C. Bradley, H.L. Anderson, J. Mater. Chem. 11 (2001) 312.
[7] G. de la Torre, P. Vazquez, F. Agullo-Lopez, T. Torres, Chem. Rev. 104 (2004) 3723.
[8] P.P. Kiran, N.K.M.N. Srinivas, D.R. Reddy, B.G. Maiya, A.S. Sandhu, A.K. Dharmadhikari, G.R. Kumar, D.N. Rao, Opt. Commun. 202 (2002) 347.
[9] P.P. Kiran, D.R. Reddy, B.G. Maiya, A.K. Dharmadhikari, G.R. Kumar, D.N. Rao, Appl. Opt. 41 (2002) 7631.
[10] P.P. Kiran, D.R. Reddy, B.G. Maiya, A.K. Dharmadhikari, G.R. Kumar, D.N. Rao, Opt. Commun. 252 (2005) 150.
[11] N.K.M.N. Srinivas, S.V. Rao, D.V.G.L.N. Rao, B.K. Kimball, M. Nakashima, B.S. DeCristofano, D.N. Rao, J. Porphyr. Phthalocya. 5 (2001) 549.
[12] A.A. Andrade, N.M. Barbosa Neto, L. Misoguti, L. De Boni, S.C. Zilio, C.R. Mendonça, Chem. Phys. Lett. 390 (2004) 506.
[13] M. Drobizhev, A. Karotki, M. Kruk, N.Zh. Mamardashvilli, A. Rebane, Chem. Phys. Lett. 361 (2002) 504.
[14] A.A. Said, C. Wamsley, D.J. Hagan, E.W. Van Stryland, B.A. Reinhardt, P. Roderer, A.G. Dillard, Chem. Phys. Lett. 228 (1994) 646.
[15] A.A. Kumar, L. Giribabu, D.R. Reddy, B.G. Maiya, Inorg. Chem. 40 (2001) 6757.
[16] L. Giribabu, T.A. Rao, B.G. Maiya, Inorg. Chem. 38 (1999) 4971.
[17] K. Kalyanasundaram, Photochemistry of Polypyridine and Porphyrin complexes, Academic Press, 1992.
[18] M. Sheik-Bahae, A.A. Said, T.H. Wei, D.J. Hagan, E.W. VanStryland, IEEE J. Quantum Electron. 26 (1990) 760.
[19] R.L. Sutherland, Handbook of Nonlinear Optics, Marcel Dekker, New York, 1996.
[20] S.V. Rao, N.K.M.N. Srinivas, D.N. Rao, L. Giribabu, B.G. Maiya, R. Philip, G.R. Kumar, Opt. Commun. 182 (2000) 255.
[21] D.C. Rodenberger, J.R. Heflin, A.F. Garito, Nature 359 (1992) 309.
[22] M. Terazima, H. Shimizu, A. Osuka, J. Appl. Phys. 81 (1997) 2946.
[23] D. Kim, A. Osuka, J. Phys. Chem. A 107 (2003) 8791.
[24] J.R.G. Thorne, S.M. Kuebler, R.G. Denning, I.M. Blake, P.N. Taylor, H.L. Anderson, Chem. Phys. 248 (1999) 181.
[25] R.K. Jain, M.B. Klein, in: R.A. Fisher (Ed.), Optical Phase Conjugation, Academic Press, New York, 1983.
[26] C. Zhan, D. Li, D. Wang, D. Zhang, Y. Li, W. Xu, Z. Lu, L. Zhao, Y. Nie, D. Zhu, Chem. Phys. Lett. 347 (2001) 410.
[27] M. Fakis, G. Tsigaridas, I. Polyzos, V. Giannetas, P. Persephonis, I. Spiliopoulos, J. Mikroyannidis, Chem. Phys. Lett. 342 (2001) 155.
[28] A.V.V. Nampoothiri, B.P. Singh, G.R. Kumar, J. Nonlinear Opt. Phys. Mater. 7 (1998) 571.
[29] S.V. Rao, D.N. Rao, J.A. Akkara, B.S. DeCristafano, D.V.G.L.N. Rao, Chem. Phys. Lett. 297 (1998) 491.
[30] G.S. He, J.D. Bhawalkar, C.F. Zhao, P.N. Prasad, Appl. Phys. Lett. 67 (1995) 2433.
[31] M. Drobizhev, A. Karotki, A. Rebane, C.W. Spangler, Opt. Lett. 26 (2001) 1081.
[32] M. Albota, D. Beljonne, J.-L. Bredas, J.E. Ehrlich, J.-Y. Fu, A.A. Heikal, S.E. Hess, T. Kogej, M.D. Levin, S.R. Marder, D. McCord-Maughon, J.W. Perry, H. Rockel, M. Rumi, G. Subramaniam, W.W. Webb, X.-L. Wu, C. Xu, Science 281 (1998) 1653.
[33] E.J. Canto-Said, D.J. Hagan, J. Young, E.W. Van Stryland, IEEE J. Quantum Electron. 27 (1991) 2274.